Representative cycle for heat pump energy flexibility evaluations - A comparative simulation study of existing day selection procedures to a new consecutive day procedure

Representative cycle for heat pump energy flexibility evaluations – A comparative simulation study of existing day selection procedures to a new consecutive day procedure

Maarten Evens[1,2], Alessia Arteconi[1,2,3]

[1]Department of Mechanical Engineering, KU Leuven, 3000, Leuven, Belgium

[2]EnergyVille, 3600, Genk, Belgium

[3]Dipartimento di Ingegneria Industriale e Scienze Matematiche, Università Politecnica delle Marche, 60131, Ancona, Italy

Abstract

Heat pumps allow to decarbonise the heating sector and to provide energy flexibility services. Hence, flexible heat pump control strategies are being developed. When testing these strategies, hardware-in-the-loop experiments using representative test cycles allow to evaluate the real heat pump behaviour. While several works investigated the representative cycle composition for retrieving the yearly energy performance, it is unclear if they can still be used for energy flexibility analysis. This paper investigates the performance of the three mainly used representative day selection procedures available in literature in presence of seven heat pump control strategies. A new approach, in which only consecutive days are used, was also evaluated. Two hydraulic configurations, i.e. with and without an energy storage between heat pump and building, and three climatic zones spread over the European Union were used in order to reach a general conclusion. Simulation results showed that approaches using consecutive days or approaches which select days based on their energy consumption can be used for the energy flexibility analysis. Though, only approaches with consecutive days were able to closely follow the operative room temperature profiles when compared to a full winter simulation due to the avoidance of abrupt temperature variations between the different days.

Keywords

Heat pump – Thermal energy storage – Energy flexibility – Hardware-in-the-loop – Testing cycles

Nomenclature

Abbreviations

BUH	Back-up heater
Clu	Day selection approach based on day clustering
DHW	Domestic hot water
Dur	Day selection approach based on duration curve/day aggregation
FF1	Flexibility factor 1
FF2	Flexibility factor 2
GHI	Global horizontal irradiation

HIL	Hardware-in-the-loop
HP	Heat pump
KPI	Key performance indicator
Mac	Day selection approach based on energies
MPC	Model predictive control
REF	Reference control strategy without energy flexibility services
RMSE	Root mean squared error
SCOP	Seasonal coefficient of performance
SoC	State-of-charge
SH	Space heating
STRAT	Energy flexible control strategy
TES	Thermal energy storage
Typ	Day selection approach based on using a typical week with consecutive days only
UFH	Underfloor heating

Symbols

A	Surface area (m²)
C	Specific heat capacity (J/kg.K)
D	Number of days (-)
D	Thickness (m)
E	Energy (J)
Err	Error (-)
L	Number of construction layers within surface m, limited to the insulated building layers and excluding the insulation layer itself (-)
m	Number of construction surfaces within a room (-)
$\dot{m}$	Mass flow rate (kg/s)
n	Number of winter months (-)
R	Number of rooms or floor levels within the simulated building (-)
S	Number of thermal energy storages (-)
SP	Spot price (€/MWh)
T	Temperature (°C)
t	Time (s)
V	Volume (m³)
X	Number of investigated flexible control strategies for a certain hydraulic configuration (-)
ρ	Mass density (kg/m³)
ζ	Factor (-)

Subscripts

air	With reference to thermal properties of air
avg	Average
$bottom$	Close to the bottom of the thermal storage
$condenser$	With reference to the heat pump condenser-side
$corr$	Correction
cum	Cumulative
$diff$	Difference between the end of the initialisation day and end of the last day within the time shortened test cycle
$elec$	Electrical
end	At the end
$FullW$	With reference to full winter period
$hyst$	Hysteresis
$inlet$	With reference to the inlet side
min	Minimum
max	Maximum
Nom	At nominal conditions
$norm$	Normalised datapoint
$orig$	Original datapoint
out	Outdoor air
$outlet$	With reference to the outlet side
$Q1$	First quartile

Q3	Third quartile
rad	Radiative
room	Room
sel	Amount that has to be selected
shift,pot	Remaining shifting potential (%)
shift,pot,red	Reduction in remaining shifting potential (%)
start	At the start
sup	Supply setpoint
th	Thermal
top	Close to the top of the thermal storage
w	With reference to thermal properties of water
7d	With reference to time shortened sequence of seven days

1. Introduction

Within the European Union, buildings account for 40 % of the energy consumption and for 36 % of the energy-related greenhouse gas emissions. Hence, improvements within the building heating and cooling systems show great potential for reaching carbon-neutrality in the EU by 2050 [1]. Thanks to their electrical grid connection, heat pumps (HPs) allow using renewable energy resources and when smartly controlled, they also allow the provision of energy flexibility services [2]. A first step in the development and analysis of these smart and flexible HP control strategies is to obtain an accurate HP model as its short-term behaviour should be well represented, including the onboard control. Indeed, several studies highlighted the shortcomings of steady-state conditions according EN 14511 [3] and EN 14825 [4] when analysing the transient HP system behaviour. By comparing several modelling approaches of the HP compressor controller and domestic hot water (DHW) prioritisation, Clauß et al. [5] investigated the importance of an accurate HP model for demand response analysis. They concluded that for short-term behaviour analysis, the HP model should well represent its transient behaviour. In addition, Evens & Arteconi [6] compared several modelling approaches for heat pumps and by gradually increasing the HP modelling complexity, they showed that most effects were visible in the short-term behaviour. They further improved and validated their short-term HP model in a hardware-in-the-loop (HIL) set-up [7] via artificially constructed load profiles.

In light of investigating the short-term HP behaviour, hardware-in-the-loop (HIL) experiments and field trials allow further development and validation of an accurate HP model as well as testing smart HP control strategies. Compared to field trials, HIL experiments ease setting equal boundary and start conditions, while different hydraulic configurations or heat emission systems can be easily tested. A pre-requirement of performing HIL experiments is composing a short, though representative, testing campaign to reduce the testing time and related costs [8]. Herein, several works already defined the selection criteria and guidelines to retrieve a representative period for annual HP performance analysis. The MacSheep project [9], [10] provided an overview of the most commonly used dynamic test methodologies for heating and cooling systems and discussed their main differences. Although the existence of several methodologies, the MacSheep project also developed a new and harmonised approach based on the combination of the existing approaches. The methodology proposed ensures an identical load provision, with the unit under test still in autonomous control as in real installations.

Furthermore, Menegon et al. [11] investigated the experimental performance characterisation of heating and cooling systems. On a whole system analysis, they applied a day clustering methodology for several combinations of two, three or four selection criteria, i.e. outdoor temperature (T_{out}), global horizontal irradiation (GHI), heating load and cooling load. They concluded that clustering days based on only T_{out} and GHI reached best agreement with the annual simulation, while scaling factors are required as the selected days for each cluster do not fully represent the cluster load energy. Similarly

to the MacSheep project, they also applied a building pre-simulation to define the load profile, for which the thermal capacity of the heat distribution system was also reduced to prevent energy shifting of high thermal inertia systems over several days. Furthermore, the authors showed that reordering the days affected the results and proposed three main solutions for which they considered the latter one as the most feasible, (1) forced energy extraction before the winter day, (2) irradiation reduction during summer days and (3) simulating the winter days before the summer days.

In addition, Mehrfeld et al. [12] formulated an experimental procedure to evaluate the yearly HP efficiency based on a time shortened testing sequence of four representative days. Within their study, days were chosen based on the representativeness of the hourly T_{out} and direct and diffuse solar irradiation. To prevent unequal thermal building mass states, a pre-simulation of ten days prior to the real testing day is simulated. From their study, it was shown that a warm – cold – warm day reordering led to the least mean deviation in the inner energy, while extrapolating the results from the test sequence to yearly performances showed better agreement for a warm – cold day reordering procedure. The authors carefully recommended to use the warm – cold sequencing procedure as they showed that the overestimation of the seasonal coefficient of performance (SCOP), due to not having the coldest days of the year, compensate for the additional state-of-charge (SoC) of thermal energy storages (TES) when using a warm – cold day order.

Analysing these yearly energy performance characterisation procedures with regard to the applicability for testing flexible HP control strategies points out several shortcomings. Firstly, using predetermined load profiles prevents charging the building during low electricity prices and shifting energy towards the next day. Even if these predetermined load profiles could be time-shifted, they would still neglect changing building heat losses when shifting room temperature setpoints. Also, working with predefined load profiles complicates the evaluation of thermal system inertia and its related energy flexibility potential as the room temperature is not directly evaluated. These system inertia issues even occurred within the MacSheep project where two different sequence lengths were tested, namely a six and twelve day sequence. In the former case, the thermal capacity of an underfloor heating system (UFH) had to be reduced to the thermal capacity of a radiator-based system as the time shift between the charged and emitted energy in the underfloor heating could not be avoided and the repeatability of the test was affected. Another difficulty when testing smart control strategies is the usage of non-consecutive days for two main reasons. Firstly, it affects the state of charge of the building when e.g. a cold day follows a warmer day and it is unclear how to deal with the stored energy within a SH TES when shifting from day n to day n+1. Secondly, using a model predictive controller (MPC) will cause the controller to make optimal use of warmer days with a lower supply temperature and to overestimate the savings potential. Finally, reaching equivalent energy states within thermal storages at the beginning and end of the test cycle is also difficult. Indeed, even if the extracted load from the storage is equal, it does not necessarily mean equal temperature levels as the flexibility strategy can change the operational schedule to shift the HP consumption to lower price periods.

In contrast with a detailed analysis of HP systems as in the previous studies, several works [13]–[16] focus on retrieving a representative period for energy system design of district heating systems, renewable energy generation planning and seasonal energy storage. Herein, representative cycles are mainly retrieved via time aggregation, where modelling simplifications are mainly required to reduce the computational complexity within optimisation problems. Hence, the applicability for investigating the experimental short-term HP behaviour of an individual heating system with regard to energy flexibility services can be questioned. Though, due to their time aggregation capabilities, these

approaches can be used to reduce the simulation time for computationally expensive problems such as optimisation problems.

In light of these shortcomings for energy flexibility analysis with HPs, this paper develops an alternative approach, in which it is proposed to not work with representative days, but to search for a typical week within the winter season to maintain consecutive days with normal temperature transitions. The first contribution is to compare the existing procedures for selecting representative days with the new approach solely relying on consecutive days in order to draw recommendations. Therefore, a comparative simulation study will be used to determine which approach fits best with regard to the energy flexibility evaluation. The second contribution of this paper is to define representative cycle requirements for experimental energy flexibility characterisation of HPs during the winter season and to investigate the necessity of post-experimental or post-simulation measures on the energy states. The analysis will be performed for the three main climatic zones within the EU and for two hydraulic configurations, namely (1) directly coupling the HP to the building without using a SH TES and (2) the existence of a SH TES between HP and building. To analyse the applicability of each representative cycle methodology, this paper also considers multiple energy flexible control strategies.

The structure for the remaining part of this paper is as follows. Section 2 provides an overview of the used methodologies for defining a representative cycle, consisting of procedures for yearly energy performance characterisation, day aggregation procedures as well as using only consecutive days. Moreover, it provides a description of the models, hydraulic configurations, energy flexible control strategies and performance indicators that were used within the analysis. Within Section 3, the selected days from each methodology will be presented at first. Afterwards, a comparison of energy flexible performance indicators for each day selection approach to a full winter period simulation will be shown. Section 4 critically reviews the results obtained and provides directions for future work. Finally, Section 5 summarises the analysis of this work into main conclusions to define a general approach for experimental energy flexibility evaluation with heat pumps.

2. Methods

This section describes the methodologies used to obtain the testing sequence requirements for smart and energy flexibility tests with HPs during the winter season (Section 2.1), followed by a description of the case study (Section 2.2) and energy flexible control strategies that were investigated (Section 2.3). Section 2.4 presents an energy correction mechanism for correcting the differences within the energy balances between the start and end of the test cycle, while Section 2.5 discusses relevant key performance indicators (KPIs) for energy flexibility analysis. To generalise the outcome for wide-scale adoption, the study was carried out for three climatic zones within the European Union as defined within EN 14825 [4]. The selected locations for the cold, average and warm climate within this paper are represented by Helsinki (Finland), Uccle (Belgium) and Athens (Greece), respectively. Based on the national weather institutes [17]–[19], it was concluded that a typical winter period ranges from December until March within Finland and from December until February in Belgium and Greece.

2.1. Determination of the “Representative flexibility cycle”

2.1.1. Sequence length

A first aspect when selecting representative days is the required sequence length. As already mentioned in the Introduction, annual performance tests generally work with six or twelve day sequences. As highlighted within the six-day approach of the MacSheep project, the thermal capacity of high thermal inertia systems had to be reduced to prevent energy shifting between different days.

To explore the full energy flexibility potential of both the HP and building and to allow the development of smart control strategies that incorporate the building behaviour, it was decided that reducing the thermal heating system capacity cannot be used. Hence, only a twelve day approach could be used, in which one day should be selected from each month. It should be noted that the goal of this paper is to evaluate the energy flexibility potential during the winter season only as switching to cooling services requires to reverse the energy state of the building and storages. Prior analysis of using only one day for each winter month showed difficulties with high thermal inertia systems and it was decided to select a seven day period. This decision was further supported by features of smart control strategies taking into account behavioural patterns throughout the week or weekend and the potential existence of personalised DHW and/or SH setpoint schedules. Prior to the seven days cycle, an additional initialisation day to even out temperature variations in the storages and heating system was used. Hence, this day cannot be used to test a flexible control strategy and should be neglected from the analysis.

2.1.2. Day selection criteria: based on energy consumption or environmental data

The second aspect is the day selection criteria, for which Haller et al. [20] distinguished two approaches, namely (1) using thermal and/or electrical energies and (2) using the environmental conditions to select the most appropriate days. In this paper three main methodologies to determine which days should be selected are adopted from literature, namely (1) an energy-based approach similar to the MacSheep project [10] (Mac), (2) a day clustering approach on environmental conditions similar to the one used by Menegon et al. [11] (Clu) and (3) a day aggregation procedure on environmental conditions as applied in [13] (Dur). In addition, a new approach by extracting a typical week of environmental conditions consisting only of consecutive days (Typ) was also investigated. Table 1 provides an overview of the investigated day selection procedures.

Table 1 – Overview of investigated day selection approaches

Acronym	Day selection approach	Initialisation day
Mac	Minimise error for directly extrapolated energy consumption	Equal to the last day within the representative test cycle
Clu	Cluster winter days into seven groups and select the days closest to the cluster centre for the representative cycle	Equal to the last day within the representative test cycle
Dur	Minimise error between duration curves of T_{out} and GHI for the full winter period and the representative cycle	Equal to the last day within the representative test cycle
Typ	Retrieve typical week with consecutive days close to the average values of T_{out} and GHI	Equal to the day chronologically prior to the selected typical week in the climatic file

2.1.3. DHW services

All approaches consider an identical DHW draw-off profile, which was generated via DHWcalc [21] and matches with the daily DHW load of the full winter period. To ensure an identical DHW load extraction for each test cycle at varying DHW inlet and outlet temperatures, an energy balance mechanism was implemented. The mechanism measures the extracted energy and closes the extraction valve when the required energy level was reached.

2.1.4. Mac: days with representative energies for direct extrapolation purposes

This approach uses a full winter simulation to search for those days within a certain month for which, the direct extrapolation of the retrieved thermal and electrical energy values of the extracted days is closest to the cumulative energy values of the considered full month within the full winter simulation. As already mentioned, the full winter period includes December, January and February for the Belgian and Greek climate, while also March is considered within the Finnish Climate. Eq. (1) represents the day selection procedure, for which the total error for direct extrapolation to the full winter period, consisting out of n winter months, is minimised. Herein, D_i represents the number of days within month i, while $D_{sel,i}$ is equal to the amount of days that have to be selected from month i. Thermal and electrical energies are represented by E_{th} and E_{elec}, respectively, in which the index avg,i represents the average consumption within month i. To obtain a total of seven days extracted from the full winter period, on average two days should be extracted from each month. To limit temperature variations between the end of the initialisation day and the last test cycle day, it was decided that the initialisation day is equal to the last day within the test cycle.

$$Err_{Mac} = \min \sum_{i=1}^{n} \left(\left| E_{elec,avg,i} - \frac{D_i}{D_{sel,i}} \cdot \sum_{l=1}^{D_{sel,i}} E_{elec,l,i} \right| + \left| E_{th,avg,i} - \frac{D_i}{D_{sel,i}} \cdot \sum_{l=1}^{D_{sel,i}} E_{th,l,i} \right| \right) \quad (1)$$

2.1.5. Clu: clustering of all winter days into seven groups

In contrast with the previous approach, this methodology does not require a prior building simulation as its clusters days based on environmental data. The clustering technique is based on the k-medoids technique in which, data is grouped into a certain amount of clusters based on their similarity. The nearest datapoint to the clusters' centre, also known as the medoid, is used. All days from the full winter period are clustered based on their daily average T_{out} and daily sum of GHI as Menegon et al. [22] concluded that clustering days based on only these inputs reached best agreement with the annual simulation. Within this paper, each climatic location used a total number of seven clusters. The authors of [22] also concluded that the medoid load of each cluster did not perfectly match the average cluster load. Therefore, they applied a scaling factor in order to compensate for the deviation between the medoid load and the average cluster load. Within this paper, the authors decided to not implement scaling factors due to the energy flexibility services that enable energy shifting between several days. If days would then be weighted according their occurrence in the full winter season, the energy consumption of day n would be overestimated, while underestimated for day n+1. Finally, dataset normalisation was applied via Eq. (2) in order to retrieve equal weights for both T_{out} and GHI. Herein, $x_{i,norm}$ and $x_{i,orig}$ represent the normalised and original individual values, while x_{min} and x_{max} represent the minimum and maximum values within the full winter period, respectively. Similarly to the Mac approach, the initialisation day is equal to the last day within the cycle.

$$x_{i,norm} = \frac{x_{i,orig} - x_{min}}{x_{max} - x_{min}} \quad (2)$$

2.1.6. Dur: day selection based on duration curve/day aggregation

Instead of clustering days into a fixed number of groups, the approach Dur implements the methodology developed by Poncelet et al. [13]. Herein, the optimisation objective is to select those days for which the duration curve is closest to the duration curve of the full winter period. Hence, the variability in occurring conditions should be better represented. Figure 1 shows an overview of the main principle, in which the optimisation objective is to minimise the red area between the duration curves for the full winter period and the selected representative period. Within this paper, the duration curves for both T_{out} and GHI were considered and were equally weighted. The outputs from the optimisation problem are the selected days with their associated weights within the representative sequence. Hence, the relevance of each selected individual day within the time

shortened sequence can be incorporated. Similarly, to the Clu approach, such a recalculation of the energy balances, costs etc. was not considered within this paper due to the thermal building mass and storages that introduce energy shifting between days. Hence, the energy flexibility analysis puts equal weight to each representative day.

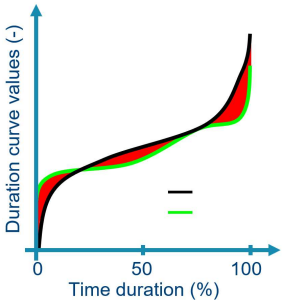

Figure 1 – Duration curve principle (Black: full winter period, Green: representative period and Red: area to minimise when selecting days). Duration curves are constructed for both T_{out} and GHI.

2.1.7. Typ: consecutive days with a close match to the environmental averages

In contrast with the previous approaches Mac, Clu and Dur, this approach uses consecutive days to achieve realistic environmental transitions between the test days. Similarly to the clustering approach, the average daily T_{out} and daily sum of GHI are used and normalised to retrieve equal weights for both variables. From the weather data file, the sequence of seven consecutive days, for which the combined root mean squared error ($RMSE$) of T_{out} and GHI between the averaged values of the seven days and the full winter months is the lowest, is selected. The combined RMSE is calculated via Eq. (3), herein the selected sequence is denoted by 7d and the reference full winter period by FullW. To enlarge the searching area for the best seven consecutive days sequence, the searching period also included the months March and November. Such an approach allows to search for a possible closer match with the full winter averages as the winter within the weather data file does not necessarily starts/ends at the first/last day of a particular month. To maintain a fully consecutive approach, the initialisation day is equal to the day within the weather file chronologically prior to the selected typical week.

$$RMSE = \sqrt{\left(T_{out,7d} - T_{out,FullW}\right)^2 + (GHI_{7d} - GHI_{FullW})^2} \quad (3)$$

2.1.8. Day ordering

Considering the transition phase between selected non-consecutive representative days, several approaches exist within literature. A first option is reordering the retrieved representative days based on their chronological appearance within the year [23], [24]. Otherwise, selected days can be reordered in several ways, e.g. warm – cold – warm or warm – cold [12], [25]. In addition to the day reordering procedures, several works [23], [25], [26] used a temperature smoothening function to further reduce outdoor temperature transitions between non-consecutive days. In this paper, an alternative approach to reduce temperature transitions between the non-consecutive approaches Mac, Clu and Dur was considered. Herein, the days were reordered based on a minimisation of the temperature changes as shown in Eq. (4), in which the start and end temperatures of each day are denoted by $T_{out,start}$ and $T_{out,end}$, respectively. Such an approach minimises unintended energy shifting within the building and storages between non-consecutive days.

$$Err = \min \sqrt{\sum_{l=1}^{D_{sel}-1} \frac{\left(T_{out,start,l+1} - T_{out,end,l}\right)^2}{D_{sel}-1}} \quad (4)$$

2.2. Case study

A two-floor detached residential single-family building with a net floor area of 194 m² was used for all three climates. To allow using the same HP within all three climates, it was ensured that the peak heating load/design heat load was identical for the building in all three climates. Though, it was decided to not largely change the building structure in order to retrieve a similar response of the building during the flexible control strategy analysis.. This lead to a design heat loss of 9.4 kW at a design temperature of -26 °C, -8 °C and 2 °C for the Finnish [27], Belgian [28] and Greek [29] climate, respectively. As indicated by Figure 2, the building is equipped with an underfloor heating system, while two system configurations were tested. Figure 2a represents a HP – building configuration without using a SH TES, while Figure 2b includes a 750 l SH TES to ease the decoupling of energy supply and demand. For the configuration without a SH TES, a heating curve is applied on the supply temperature to the underfloor heating system. In case of using a SH TES, a heating curve is applied on the HP and underfloor heating system supply temperature as well as on the SH TES temperature boundaries. Furthermore, a small system inertia storage of 25 l was used as prescribed by the HP manufacturer when not using a SH TES between HP and building. The considered HP is a Daikin type EGSAX06D9W [30] with a nominal thermal and electrical power of 11.89 kW_{th} and 1.91 kW_{elec} at a nominal building supply water temperature of 37 °C. Also, the HP is equipped with a 3 kW back-up heater (BUH), which is mainly used for legionella bacteria growth prevention within the DHW storage. Simulations with a 60 seconds time step are performed within Modelica [31], while an experimentally validated short-term behaviour HP model from a previous work was used [7].

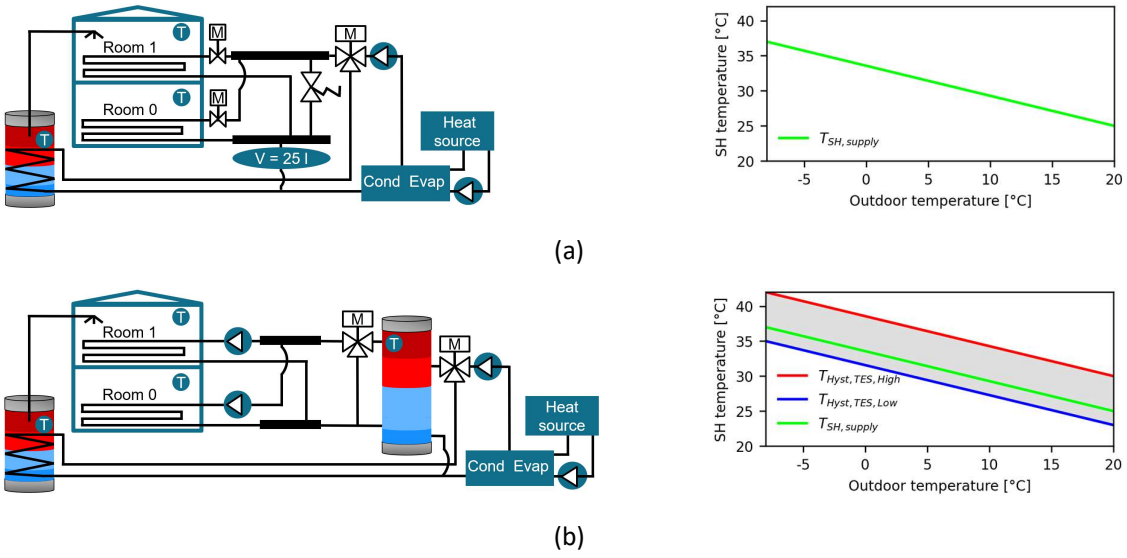

Figure 2: HP – building connection with applied heating curves: (a): without SH TES and (b): with SH TES. Within the heating curves, Green: supply temperature to the underfloor heating system, red = SH TES upper temperature hysteresis & HP supply temperature into the TES, blue = SH TES lower temperature hysteresis.

2.3. Energy flexible control strategies

As highlighted by Fischer & Madani [32], smart HP control strategies can consider many different input signals. Within this paper, a demand response flexible control strategy has been selected, based on Belgian day-ahead prices [33]. Hence, selecting a relevant period from the electricity tariff is also required. The volatility and spread of the electricity prices have to be well represented, for which the evaluation criteria were the minimum and maximum price, the quartile ranges and average deviation. From the full winter period, that sequence for which the average deviation and price difference between the first and third quartile were closest to the values of the full winter period was extracted.

By using these criteria, the dynamic price trend and corresponding flexible control strategy response throughout the test sequence should well cover the full winter period behaviour. Table 2 and Figure 3 show the differences between the full winter price data and the selected representative price sequence. It should be noted that the flexible control is deactivated during the initialisation day to allow the system to reach normal operating conditions.

Table 2 – Dynamic tariff characteristics of full winter period and representative cycle

	Full winter period	Selected short sequence period
Minimum [€/MWh]	-31.82	18.22
First quartile [€/MWh]	37.45	46.99
Second quartile (median) [€/MWh]	47.64	58.40
Third quartile [€/MWh]	58.33	67.43
Maximum [€/MWh]	134.28	90.49
Average deviation [€/MWh]	12.79	12.77

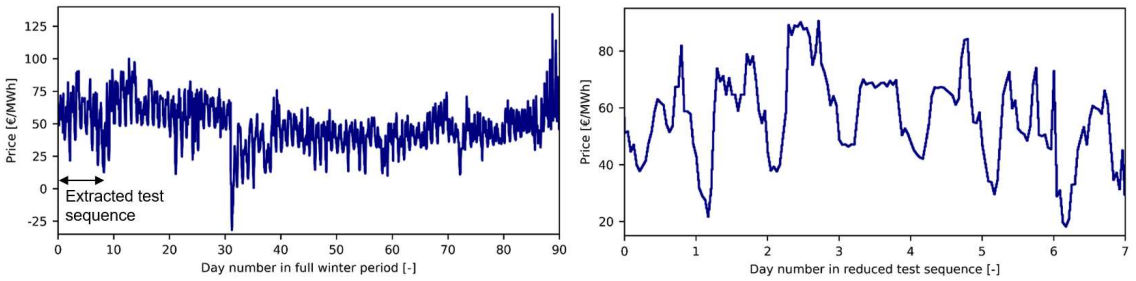

Figure 3 – Dynamic tariff graphical comparison of full winter period (a) and representative cycle (b)

For the hydraulic configuration without a SH TES (Figure 2a), a total set of three energy flexible control strategies (STRAT) were considered, while only two energy flexible control strategies were investigated for the HP – SH TES – building configuration (Figure 2b). Table 3 and Table 4 show a control strategy overview for both hydraulic configurations, including the reference control without energy flexibility services (REF). In the context of flexible HPs, Lindahl [34] distinguished direct and indirect HP control approaches. Within direct control approaches, the control directly acts on the compressor speed and the back-up heater power. Within indirect control approaches, mainly temperature setpoint adjustments or temperature sensor override functions are used to obtain the requested change in electrical HP behaviour. Except for STRAT3, all strategies act on the temperature setpoints of DHW/SH TES services, room thermostat and SH supply temperature and hence, change the operational HP behaviour rather indirectly. Within STRAT3, a direct control approach by directly acting on the HP power consumption was also tested. In what follows, the indirect control approaches will be presented, followed by the direct control approach.

Considering indirect control algorithms, Table 3 and Table 4 show a control strategy overview for both hydraulic configurations of Figure 2, with their respective reference control strategy. Herein, the energy flexible control strategies use a dimensionless flexibility factor (FF) to determine how the temperature setpoints should respond to a certain change in the electricity price. In this regard, two

different approaches were used and are shown in Eq. (5) and (6). Herein, the momentary, minimum, maximum, average, first quartile and third quartile spot prices for each day are denoted by SP, SP_{min}, SP_{max}, SP_{avg}, SP_{Q1} and SP_{Q3}, respectively. The approaches differ in their response to variations within the electricity price. Preliminary analysis showed that using the daily first and third quartile prices within *FF2* instead of the minimum and maximum daily prices in *FF1* approaches, allows a faster response to changing electricity prices. Therefore, it could be concluded that a similar electricity cost reduction with less comfort violation could be reached for *FF2* approaches. Hence, a smaller room temperature setpoint variation range for *FF2* approaches to limit the impact on the thermal comfort was applied.

$$FF1 = \begin{Bmatrix} if\ SP \geq SP_{avg}: \frac{SP - SP_{avg}}{SP_{max} - SP_{avg}} \\ if\ SP \leq SP_{avg}: \frac{SP - SP_{avg}}{SP_{avg} - SP_{min}} \end{Bmatrix} \quad (5)$$

$$FF2 = \left(\max\left(min\left(\frac{SP - SP_{Q1}}{SP_{Q3} - SP_{Q1}}\ ; 1\right)\ ; 0\right) \cdot 2\right) - 1 \quad (6)$$

In addition to room temperature setpoint variations, also an adjustment of the heating curve for the UFH system was applied, accomplished by incorporating the new room temperature setpoint via Eq. (7) for STRAT1 or via incorporation of the factor *FF2* for STRAT2 .

$$T_{SH,sup,i} = T_{room,i} + \left(MAX\left(0\ ;\ \frac{T_{room,i} - T_{out,i}}{T_{room,REF} - T_{out,Nom}}\right)\right) \cdot \left(T_{SH,sup,Nom} - T_{room,REF}\right) \quad (7)$$

Herein:

- $T_{SH,sup,i}$: SH supply temperature setpoint at hour i
- $T_{room,i}$: room temperature setpoint at hour i
- $T_{room,REF}$: room temperature setpoint within reference control strategy, i.e. 20 °C
- $T_{out,i}$: outdoor temperature at hour i
- $T_{out,Nom}$: outdoor temperature at nominal conditions

From Table 3 and Table 4, it can also be seen that the room and/or DHW thermostat states can be reset to an on- or off-state. In this regard, the flexible control strategy tries to force the thermostat into a certain state in favour of a certain flexible behaviour. A normal thermostat only changes its state after exceeding the setpoint plus or minus the temperature hysteresis/dead band. Herein, the flexible control strategy overrules the measured temperature for only one second with a too low or too high temperature if the desired action of the HP is an on-state or off-state, respectively. Therefore, the thermostat will automatically change its state to the desired flexible response. After this one second overruling interval, the actual measured temperature is again considered as an input to the thermostat. If the measured temperature is then within the allowed temperature hysteresis, the room thermostat will hold its new state and provide the desired flexible response. In the other case, the thermostat will again change its state in order to cover the thermal comfort of the inhabitants and therefore it will neglect the flexibility request.

Finally, DHW services were also considered energy flexible. Within STRAT1, the original DHW TES temperature range was maintained to prevent charging to higher DHW TES temperatures, while the DHW thermostat reset allows to charge the DHW TES at the cheapest two time slots of each individual day. In contrast, STRAT2 charges to higher DHW temperatures after potentially large DHW draw-offs,

364 while a reduction of the setpoint during the remaining period promotes charging the DHW TES during
365 low electricity price periods.

366 *Table 3 – Control strategy overview for a hydraulic configuration without using a SH TES between HP and building*

Characteristic	REF & STRAT3	STRAT1	STRAT2
Setpoint T_{room}	*20 °C*	*20 °C - 0.75 · FF1*	*20 °C - 0.25 · FF2*
Hysteresis T_{room}	*± 0.50 °C*	*± 0.25 °C*	*± 0.25 °C*
Reset room thermostat	N.A.	N.A.	If setpoint T_{room}: • Increases: *reset to on-state* • Decreases: *reset to off-state*
SH supply temperature	*UFH heating curve*	*UFH heating curve*, adjusted by new T_{room} setpoint via Eq. (7)	*UFH heating curve – 1.5 · FF2*
DHW TES temperature range and control	*42 – 47 °C*	If current hour is cheapest hour in (00:00 – 12:00) or (12:00 – 24:00): • *Reset to on-state* • *42 – 47 °C* else: • *42 – 47 °C*	If current hour is cheapest hour in (00:00 – 06:00) or (11:00 – 17:00): • *45 – 50 °C* else: • *40 – 45 °C*

367

368 *Table 4 – Control strategy overview for a HP – SH TES – building configuration*

Characteristic	REF	STRAT1	STRAT2
Setpoint T_{room}	*20 °C*	*20 °C - 0.75 · FF1*	*20 °C - 0.25 · FF2*
Hysteresis T_{room}	*± 0.50 °C*	*± 0.25 °C*	*± 0.25 °C*
Reset room thermostat	N.A.	N.A.	If setpoint T_{room}: • Increases: *reset to on-state* • Decreases: *reset to off-state*
SH supply temperature	*UFH heating curve*	*UFH heating curve*, adjusted by new T_{room} setpoint via Eq. (7)	*UFH heating curve – 1.5 · FF2*
Upper SH TES temperature	*UFH heating curve + 5 °C*	*UFH heating curve -2 · FF1 + 3 °C*	*UFH heating curve + 5 °C*
Lower SH TES temperature	*UFH heating curve – 2 °C*	*Upper SH TES temperature – 3 °C*	*UFH heating curve – 2 °C*
HP supply temperature	*Upper SH TES temperature*	*Upper SH TES temperature*	*Upper SH TES temperature*
DHW TES temperature range and control	*42 – 47 °C*	If current hour is cheapest hour in (00:00 – 12:00) or (12:00 – 24:00): • *Reset to on-state* • *42 – 47 °C* else:	If current hour is cheapest hour in (00:00 – 06:00) or (11:00 – 17:00): • *45 – 50 °C* else: • *40 – 45 °C*

		• *42 – 47 °C*	

In contrast with the indirect control approaches on temperature setpoints of SH and DHW services, an electrical HP power limitation interface was also tested in the case STRAT3, solely for the hydraulic configuration without a SH TES between HP and building. The decision to not apply a power limitation for the hydraulic configuration with a SH TES was based on the observed operational HP behaviour. When applying a SH TES between HP and building, the modulation capabilities of the HP are less used due to the SH TES thermostat control. Herein, the HP remains completely off during the SH TES discharging cycle, in which setting a stricter or even less strict power limitation constraint does not cause any change in the HP status. In case of SH TES charging cycles, it could be seen that the HP is mainly working at full load conditions. Herein, the thermal stratification within the SH TES causes a low HP return temperature, while the HP outlet temperature should be high enough to ensure a sufficiently high SH TES inlet temperature. Such an approach allows a fast recovery of the SH TES temperature near the water extraction port that provides supply water to the building. If a power limitation during these charging cycles near full load conditions would be introduced, a reduction in the inhabitant's thermal comfort could therefore be expected. Hence, it was decided to not use a power limitation control approach when using a SH TES between the HP and building.

In cases when not using a SH TES between HP and building, the HP modulation capabilities cause the HP to be mainly in an on-status. Herein, setting a power limitation constraint directly changes the operational HP behaviour towards the requested power. It should be noted that temperature setpoints within STRAT3 are equal to the reference control setpoints without energy flexibility services as shown within Table 3, while *Figure* 4 shows the pseudo-code of the applied direct control strategy The applied interface limits the electrical HP power to three discrete levels. Each day is divided within four slots, i.e. a first slot containing 40 % of the lowest prices and the remaining slots containing each 20 % of the prices. During low prices, no power limitation was activated, while the power limitation was (un)tightened if prices crossed predetermined levels. Both DHW and SH comfort were incorporated via overruling possibilities.

Define Power Limitation level as PowLim:
- PowLim1 = 0.50 kW_{elec}
- PowLim2 = 0.75 kW_{elec}
- PowLim3 = 1.50 kW_{elec}

Retrieve spot prices (SP) for the full day

Define Spot Price Limitation level as SPLim:
- SPLim1 = SP that is exceeded for 60 % of the day
- SPLim2 = SP that is exceeded for 40 % of the day
- SPLim3 = SP that is exceeded for 20 % of the day

Define Requested Power Limitation level as PowLimReq:
- if SP > SPLim3 ➔ PowLimReq = PowLim1
- else if SP > SPLim2 ➔ PowLimReq = PowLim2
- else if SP > SPLim1 ➔PowLimReq = PowLim3
- else ➔ no power limitation is requested ; return to normal operation

Check for comfort / health constraints and communicate final control decision to the HP system:
- if room temperature < (setpoint - 1 °C) ➔ return to normal operation due to SH discomfort
- else if anti-legionellae cycle active ➔ return to normal operation due to anti-legionellae cycle
- else if DHW charging cycle and DHW temperature < 40 °C ➔ return to normal operation due to DHW discomfort
- else if DHW charging cycle and DHW temperature ≥ 40 °C ➔ maximum power limitation is PowLim3 due to DHW discomfort
- else ➔ send PowLimReq directly to the HP system

Figure 4 – Pseudocode of direct HP control algorithm

2.4. Reaching comparable start and end conditions

In the literature, several works show that a reordering of the selected days can already reduce the remaining energy state difference between the start and end of the representative test cycle. Though, correctly analysing smart control strategies in short sequences requires a correction mechanism to fully incorporate the difference in state-of-charge of the building and TES, especially if a large energy content can be stored. Indeed, energy flexible control strategies enable energy shifting by changing the operational HP behaviour, while comparison of the final energy consumption or cost over several smart strategies requires a comparable start- and end-point. Herein, fixed load profiles do ensure an identical load extraction, but do not necessarily lead to an identical state-of-charge of the building and thermal storages. Within this context, preliminary reference simulation analysis showed mainly one or two underfloor heating cycles per day when using variable capacity HPs. Hence, when investigating control strategy improvements, small energy state differences reversed the final strategy conclusion when analysing its effectiveness. Furthermore, comparing the inherent energy flexibility of different hydraulic configurations or heat emission systems requires equal energy states.

As the previously mentioned methodologies do not allow to perform post-simulation corrections, an alternative approach based on defining the energy state difference between the end of the initialisation day and end of the last day is considered in this paper. For this reason, both the energy costs and energy consumptions are corrected by using a correction factor ζ_{corr}. To determine ζ_{corr}, a prior requirement is calculating the difference between the thermal energy stored within the storages and the building after the initialisation day and after the full cycle of eight days via Eq. (8). It has to be noted that the general formulation of Eq. (8) allows to incorporate all room elements such as walls, floor, roof, windows, doors, … Within this paper, the energy stored within doors and windows is neglected due to the limited energy storage potential. Depending on the level of detail within the building simulation, the variable r can represent the number of rooms or number of floor levels within the building. Furthermore, when using multi-level buildings with active heating layers such as an underfloor heating system, the energy stored within the intermediate construction layers should be carefully treated. Preliminary result analysis on the occurrence of insulation layers between two adjacent zones, equipped with an active heating layer, showed that the building layers below the insulation layer were still in initialisation phase at the end of the initialisation day. Indeed, the heat transfer with an underfloor heating is mainly going upwards and the insulation layers limit the heat transfer to the lower located rooms. To prevent wrong estimations of the state-of-charge, two main solutions are proposed. Firstly, setting a realistic start temperature of all active heating construction layers to reduce the transient conditions. Secondly, within multi-level buildings, the temperature of the ceiling cannot be fully used if an underfloor heating system is present at the next floor level. Within these circumstances, it is proposed to determine the percentage of heat transfer from the underfloor heating that is moving downwards under design conditions, based on the thermal resistance of each floor construction layer. The obtained factor should then be multiplied with the related layer within the procedure of Eq. (8). Finally, the last part of Eq. (8) considers an average TES temperature to determine the potential change in state-of-charge for a total of s storages. It was decided to use temperature measurements of two different storage height locations to incorporate the thermal stratification within the TES and to better represent the real state-of-charge of the thermal storages.

$$E_{th,diff} = \sum_{i=1}^{r}\left(\sum_{j=1}^{m}\left(A_j \cdot \left(\sum_{k=1}^{l}(d_k \cdot \rho_k \cdot c_k)\right)\right) \cdot \left(T_{rad,end,m} - T_{rad,start,m}\right) + V_{air,i} \cdot \rho_{air} \cdot c_{air} \cdot \left(T_{air,end,i} - T_{air,start,i}\right)\right) + \sum_{q=1}^{s}\left(V_q \cdot \rho_w \cdot c_w \cdot \frac{\left(T_{q,top,end} + T_{q,bottom,end}\right) - \left(T_{q,top,start} + T_{q,bottom,start}\right)}{2}\right) \quad (8)$$

After calculating the energy state difference, the total thermal energy provided by the HP is used to retrieve the final correction factor via Eq. (9). Herein, the total thermal energy provided at the condenser-side and by the potential back-up heater (BUH) are calculated.

$$\zeta_{corr} = \frac{E_{th,condenser} + E_{th,BUH} - E_{th,diff}}{E_{th,condenser} + E_{th,BUH}} \quad (9)$$

Afterwards, the thermal energies, electrical energies and energy costs over the representative week without the initialisation day are multiplied by the correction factor as shown in Eq. (10). Herein, E_{KPI} represents the energetic KPI that has to be corrected, calculated from the end of the initialisation day to the end of the last day of the representative cycle.

$$E_{KPI,corr} = \zeta_{corr} \cdot E_{KPI} \quad (10)$$

Unless clearly described, all energy indicators within this paper already represent the corrected indicators, obtained via the post-processing energy correction mechanism.

2.5. Energy flexibility performance indicators

Finally, a selection of relevant KPIs for energy flexibility analysis has to be made. As already indicated, the first day within the representative cycle acts as initialisation day to even out temperature variations and is excluded from further analysis. For the remaining seven days within the cycle, several performance indicators can be calculated, for which Table 5 shows an overview divided into KPIs focussing on the thermal comfort, energy performance and HP operation.

Table 5 – Overview of energy flexibility performance indicators divided into: Thermal comfort, Energy performance and HP operation

Thermal Comfort	Energy Performance	HP operation
Air room temperature distribution	Thermal energy	Number of DHW cycles
Operative room temperature distribution	Electricity consumption	Number of compressor cycles
DHW temperature distribution	SCOP	Compressor on-time
	Billing cost	Average compressor speed
	Remaining energy shifting potential	

The air and operative room temperature distributions as well as the DHW temperature distribution are used to visualise the end-users' thermal comfort. Furthermore, the analysis includes the condenser energy, BUH energy, electricity consumption, SCOP, number of compressor cycles, DHW cycles, average compressor modulation and electricity costs. Results include both absolute and relative KPIs. Absolute KPIs are obtained by direct extrapolation via the number of days, while relative KPIs are obtained by comparison to the reference control strategy without energy flexibility services. To further investigate the overall performance of a specific day selection approach, the root mean squared error ($RMSE$) for the relative KPIs was calculated via Eq. (11). Herein, i represents the evaluated flexible strategy, denoted by $STRAT_i$, out of a total of X flexible control strategies within a certain hydraulic configuration. The representative sequence is denoted by 7d and the full winter period simulation by FullW. The $RMSE$ values can be expressed as a percentage due to the relative comparison to the reference case without flexibility services, denoted by REF.

$$RMSE = 100 \cdot \sqrt{\frac{\sum_{i=1}^{X}\left(\frac{KP\ _{7d,STRA\ _i} - KPI_{7d,REF}}{KPI_{7d,REF}} - \frac{KPI_{\mathrm{FullW},STRAT_i} - KPI_{\mathrm{FullW},REF}}{KPI_{\mathrm{FullW},REF}}\right)^2}{X}} \quad (11)$$

At the level of electricity costs, a single energy billing cost is highly affiliated to the occurring price levels and it does not provide an indication on the remaining potential for control strategy improvement nor does it show how exactly the cost reduction was achieved. To overcome these issues, two other indicators were considered. (1) A first approach is similar to histograms and ranks the electricity prices of each time slot within a single day from low to high prices. Then, this ranking is divided into eight price ranges, each containing 12.5 % of the price data set, by selecting seven price levels. Each price range slot is also coupled to a cumulative electrical energy counter $E_{elec,cum,i}$, which represents the total HP electricity consumption within the affiliated price range i, with $i = 1$ for the lowest price range and $i = 8$ for the highest price range. Thereafter, for each time slot of the original price data set, the momentary price is compared to the seven price levels. The HP electricity consumption of each particular time slot is then added to the electricity consumption counter of the valid price range. It has to be noted that this procedure is considered for the full test cycle, in which the seven price levels are determined on a daily basis. Hence, instead of retrieving eight factors for each individual day, all days are combined into eight counters. By dividing all these eight counters by the total HP electricity consumption over the complete test cycle, the share of the HP electricity consumption $E_{elec,share,i}$ over the electricity prices can be seen. While such an approach leads to eight individual factors, the second approach (2), which is mainly used in this paper, combines the eight electricity consumption counters into a single factor $E_{shift,pot}$, as shown in Eq. (12), which represents the remaining energy shifting potential. This factor compares the final HP electricity consumption distribution to the most ideal distribution. If all HP electricity consumption occurs during the cheapest price range, then the remaining energy shifting potential would be 0 %, while the factor would be equal to 100 % if all electricity consumption occurred within the most expensive price range. Although a 0 % value is highly unlikely as it assumes that the HP is only activated during the cheapest three hours of each day, this factor eases the comparison of control strategy effectiveness when improving the strategy as it is less sensitive to price changes between several days. It has to be noted that in case of local energy production, the remuneration for a net electricity injection has to be carefully considered when different price rates are used for a net energy consumption and production.

$$E_{shift,pot} = 100 \cdot \frac{\left(\frac{\sum_{i=1}^{8} E_{elec,share,i} \cdot \frac{i}{8}}{\sum_{i=1}^{8}\left(1 - \frac{i-1}{8}\right)}\right) - \frac{\frac{1}{8}}{\sum_{i=1}^{8}\left(1 - \frac{i-1}{8}\right)}}{\frac{1}{\sum_{i=1}^{8}\left(1 - \frac{i-1}{8}\right)} - \frac{\frac{1}{8}}{\sum_{i=1}^{8}\left(1 - \frac{i-1}{8}\right)}} \quad (12)$$

3. Results

In this section, results will be presented in three main sub-sections. Firstly, the selected days and the related coverage of the full winter period for each representative day selection methodology will be presented. Secondly, the day selection approaches will be compared over the three European climate zones with respect to the investigated flexible control strategies. Finally, an evaluation of the energy correction mechanism will be discussed.

3.1. Comparison of day selection approaches on environmental data

Figure 5 – Figure 7 provide an overview of the environmental condition spread for the different day selection approaches compared to the full winter period, for the Finnish, Belgian and Greek climate, respectively. Moreover, Table 6 provides the average values of T_{out} and GHI for all approaches

compared to the full winter period as well as the $RMSE$ values retrieved via Eq. (3). The consequence of selecting a fully consecutive typical week within the selection procedure Typ can be seen in the scatter plots for T_{out} and GHI, for which both the coverage of more extreme conditions and the first – third quartile of the boxplots are reduced. Therefore, the consecutive approach Typ represents a rather mild winter week without large variations of environmental conditions. Comparison with the approaches Clu, Dur and Mac shows the improved ability of Clu, Dur and Mac for covering a larger variety of environmental conditions as these approaches do not require fully consecutive days and are able to select days throughout the full winter season. Though, the scatter plots also show that for milder climates, i.e. Belgium and Greece, the selected days within the consecutive approach Typ can also cover a wider variety of environmental conditions and reach a similar coverage area as the non-consecutive approaches. Within this context, coverage areas are defined as the comparison of the spread of the selected days within the scatter plots compared to the full winter period. Furthermore, Clu, Mac and Dur show a similar coverage area for the different environmental conditions within the scatter plots, while the procedures consider a completely different approach by using the final energy consumption levels within Mac and only the environmental conditions within Clu and Dur. Hence, a strong correlation between the final energy consumption and environmental conditions of T_{out} and GHI can be proven. In addition, when using energy consumption levels to select representative days within the approach Mac, consistently lower average GHI values for all three climates can be found, while within the Finnish climate also a larger first – third quartile range for T_{out} can be noticed, when compared to the full winter period. Furthermore, comparison of Clu and Dur shows an improved boxplot range for T_{out} within Dur, while the boxplot range of Clu shows a better match with the full winter data for GHI. Hence, investigating smart HP control strategies acting on PV panels or high thermal inertia buildings with large window areas can lead to different results. Finally, comparison of the $RMSE$ values within Table 6 does not show a preferred approach when only considering the environmental conditions. Indeed, the clustering approach Clu shows less deviation for the average climate of Belgium, while only using consecutive days within Typ showed the lowest $RMSE$ for the cold climate of Finland and warm climate of Greece. Finally, the approach Dur shows the highest deviations of all four approaches within all climates, which can also be seen from the median values within the boxplots of Figure 5 – Figure 7.

Table 6 – Comparison of ($T_{out,7d}$; GHI_{7d}) to ($T_{out,FullW}$; GHI_{FullW}) for the day selection approaches

Approach	Finland	Belgium	Greece
Mac [°C ; Wh/m².day]	(-3.60 ; 614)	(3.66 ; 609)	(10.56 ; 1993)
Clu [°C ; Wh/m².day]	(-3.79 ; 970)	(4.46 ; 783)	(10.44 ; 2454)
Dur [°C ; Wh/m².day]	(-4.74 ; 511)	(2.62 ; 507)	(9.76 ; 1855)
Typ [°C ; Wh/m².day]	(-2.70 ; 824)	(3.95 ; 637)	(10.51 ; 2143)
FullW [°C ; Wh/m².day]	(-3.33 ; 784)	(4.02; 784)	(10.41 ; 2211)
$RMSE$ Mac [%] according Eq. (3)	5.37	8.62	6.25
$RMSE$ Clu [%] according Eq. (3)	6.13	2.70	6.78
$RMSE$ Dur [%] according Eq. (3)	10.95	14.03	11.58
$RMSE$ Typ [%] according Eq. (3)	4.10	5.82	1.95

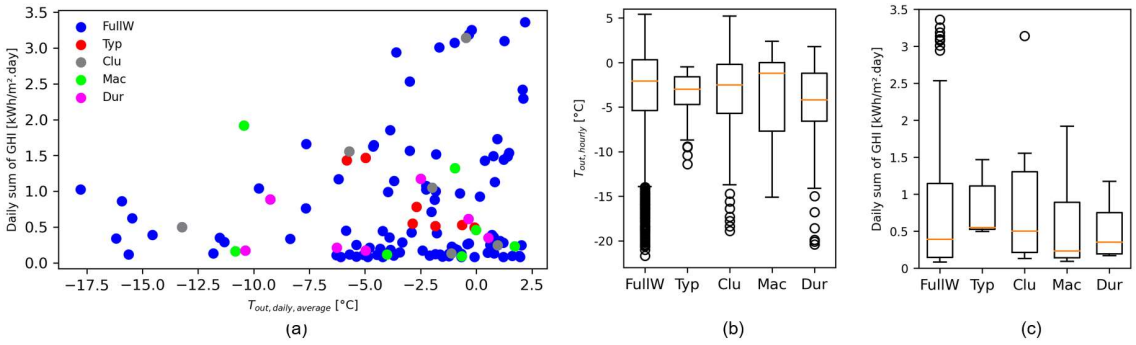

Figure 5 – Comparison of day selection approaches for Finland: (a) spread of (T_{out} ; GHI), (b) boxplot of hourly variation of T_{out} and (c) boxplot of daily sum of GHI

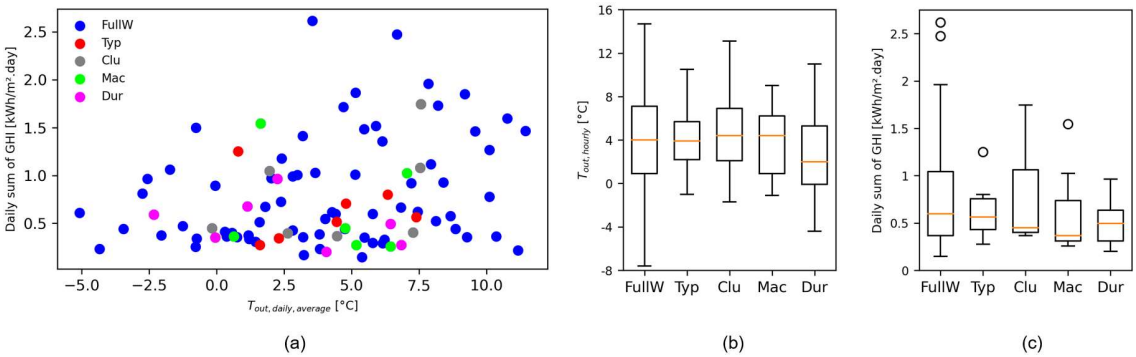

Figure 6 – Comparison of day selection approaches for Belgium: (a) spread of (T_{out} ; GHI), (b) boxplot of hourly variation of T_{out} and (c) boxplot of daily sum of GHI

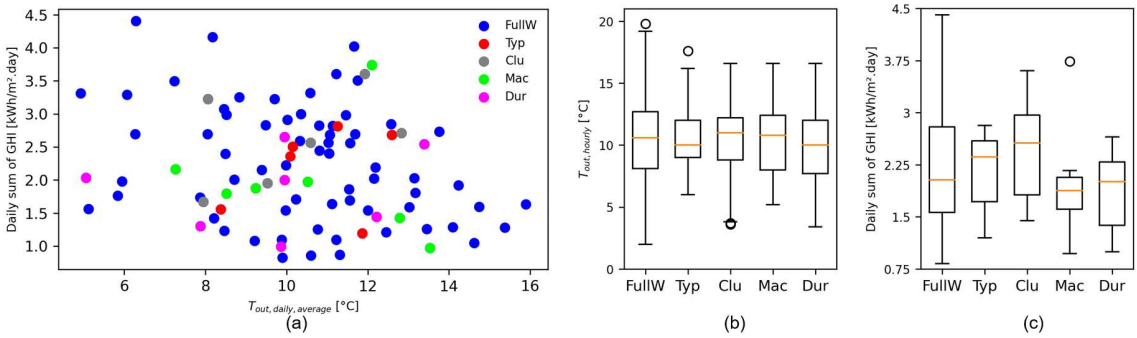

Figure 7 – Comparison of day selection approaches for Greece: (a) spread of (T_{out} ; GHI), (b) boxplot of hourly variation of T_{out} and (c) boxplot of daily sum of GHI

3.2. Comparison of day selection approaches within energy flexible control strategies

This section compares the day selection approaches for both hydraulic configurations of Figure 2. To easily investigate the potential effects of a different hydraulic configuration on the applicability of the day selection approaches, both configurations will be shown next to each other. Herein, the hydraulic configuration without a SH TES between HP and building will be shown on the left and the HP – SH TES – building configuration on the right. Figure 8 shows the energy-related KPI for the Finnish, Belgian and Greek climate.

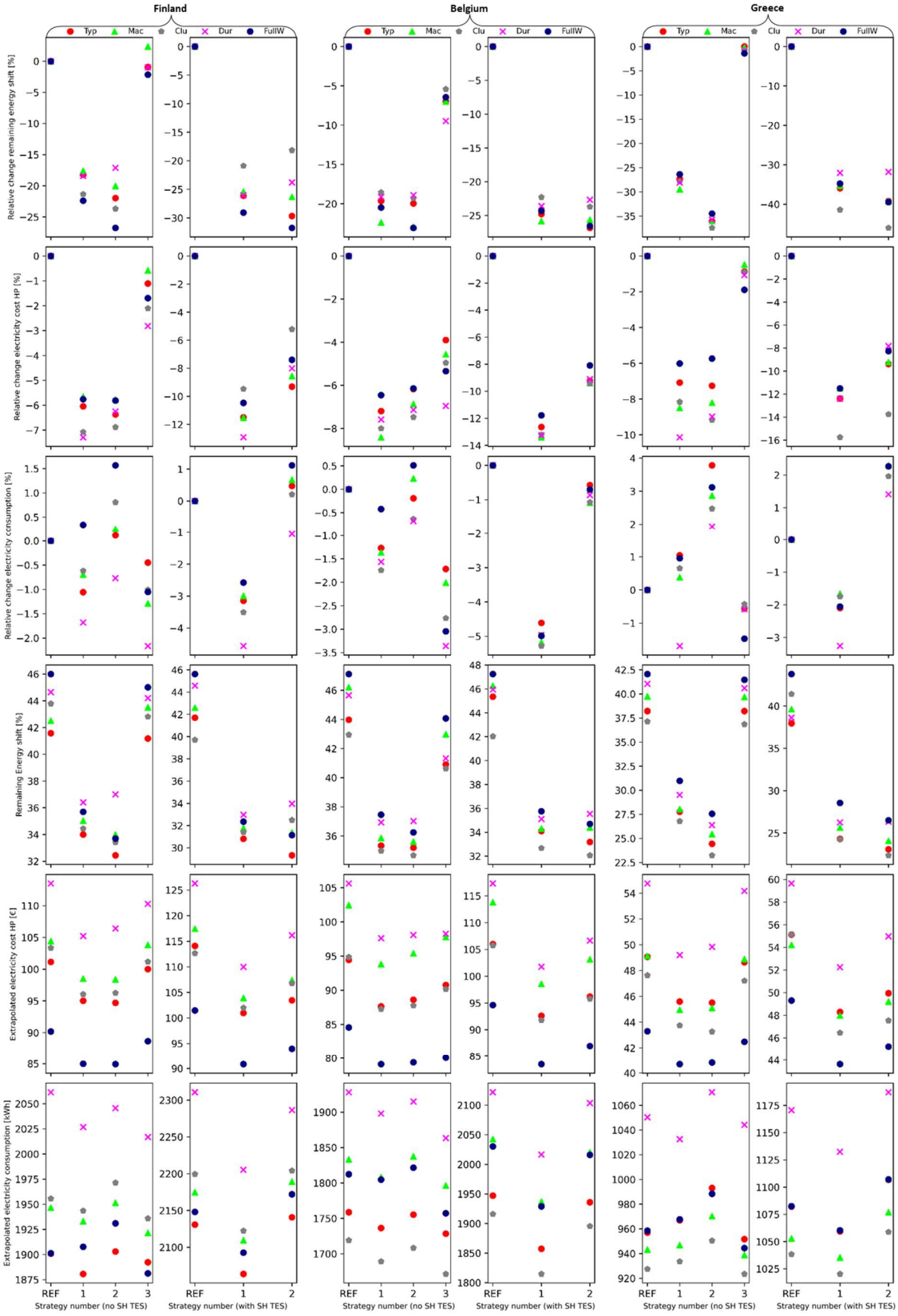

Figure 8 – Relative and absolute energy flexible KPIs: remaining energy shifting potential, electricity costs and electricity consumption. For each climatic zone: left: no SH TES between HP and building, right: HP – SH TES – building configuration

From Figure 8, it can be concluded that both the Clu and Dur day selection approaches do not show good agreements for the relative KPIs (reduction in the remaining energy shifting potential ($E_{shift,pot,red}$), energy costs and electricity consumption) when compared to the full winter simulations. Herein, agreements refer both to individual point-to-point comparison between the day selection procedure and full winter simulation for a single control strategy as well as when changing from strategy, e.g. from STRAT1 to STRAT2. For instance, when using a SH TES between HP and building, clustering days within Clu underestimates the reduction in energy costs and $E_{shift,pot,red}$ for the Finnish climate, while it overestimates the same indicators within the Greek climate. Moreover, STRAT2 shows a lower reduction in $E_{shift,pot,red}$ when compared to STRAT1 for the Finnish climate, while the full winter simulations show a higher reduction for STRAT2. Also, when not using a SH TES between HP and building, Clu does show higher deviations for $E_{shift,pot,red}$ within the Finnish climate, for which the improvement for $E_{shift,pot,red}$ when switching from STRAT1 to STRAT2 is less pronounced.

Similarly to clustering days within Clu, also the duration curve approach Dur shows higher deviations. For both hydraulic configurations within the Finnish climate, STRAT2 performs worse than STRAT1 for both $E_{shift,pot,red}$ and the energy costs, while the full winter simulations show a further reduction in energy costs and $E_{shift,pot,red}$ for STRAT2. For the Belgian climate, the relative KPIs for STRAT3 show the largest deviations for the Dur approach when compared to the full winter simulation when not using a SH TES. Within the Greek climate, Dur also shows opposite trends for the energy costs and electricity consumption. Indeed, for the hydraulic configuration without a SH TES, STRAT1 shows a 1 % electricity consumption decrease for Clu, while the full winter simulation shows an increase of 3 % when compared to the reference control strategy REF. The analysis of the extrapolated values for the energy costs and electricity consumption points out that the Dur approach overestimates both indicators for all three climates and for both hydraulic configurations. Considering the clustering approach Clu, deviations of the extrapolated values are smaller, while the approaches Mac and Typ mainly perform better. Hence, it can be concluded that both Clu and Dur approaches cannot be used when analysing energy flexible control strategies. A potential reason can be found within the attempt to cover a large variety in environmental conditions, which does not correspond to the full winter trend when days cannot be weighted according to their occurrence within the full winter period due to the energy shifting between different days.

Analysis of the consecutive approach Typ and the energy-based approach Mac provides similar results for the relative KPIs of $E_{shift,pot,red}$, the energy costs and electricity consumption, for which most differences can be seen for colder climates. Indeed, results within the Greek climate show only small variations to the full winter simulation. Moreover, when using a SH TES between the HP and building, both Typ and Mac show good agreements for the aforementioned relative KPIs for all three climates, mainly better than the configuration without a SH TES. Herein, the main reason can be found in the usage of a SH TES, which separates the HP operation into time slots near full load operation during the charging process and an off-state for the remaining time. In addition, the daily trend of lower outdoor temperatures during the night can be covered by both the building and SH TES. Considering the usage of a SH TES in the Finnish and Belgian climate, results show a slightly better agreement for Mac when considering the directly extrapolated electricity consumption over the full winter season, while $E_{shift,pot,red}$ is better represented by the consecutive days approach Typ. Moreover, for the Belgian climate, small differences for both approaches Mac and Typ can be seen for $E_{shift,pot,red}$, the relative change within the electricity consumption and electricity cost. Though, these differences remain rather small and can be related to the error when composing the reference period as shown within Table 6.

In contrast, slightly larger variations between Typ and Mac can be noticed when not using a SH TES between HP and building due to the more continuous operation of the HP, in which the HP modulation capabilities are better exploited. Both approaches consider an electricity consumption decrease for STRAT1 within the Finnish climate, while the full winter simulation shows a small increase. Again, the deviation is rather small and can be related to the reference period composition error. Also within the directly extrapolated values for the electricity consumption and cost, both approaches perform well.

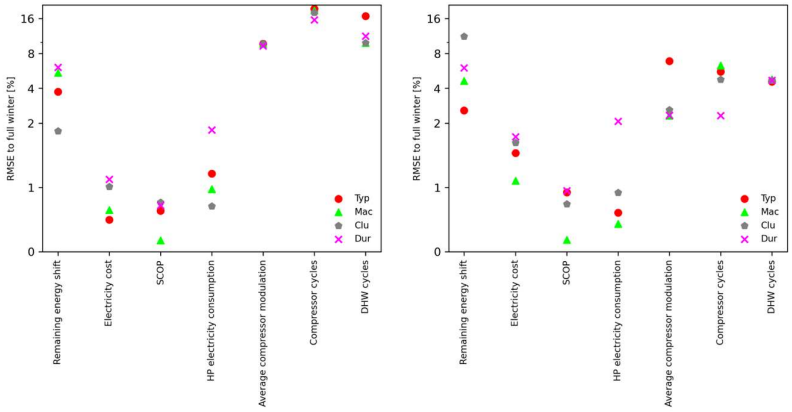

Figure 9 – RMSE according Eq. (11) for relative KPIs compared to full winter simulation for the Finnish Climate. Left: no SH TES between HP and building, right: HP – SH TES – building configuration

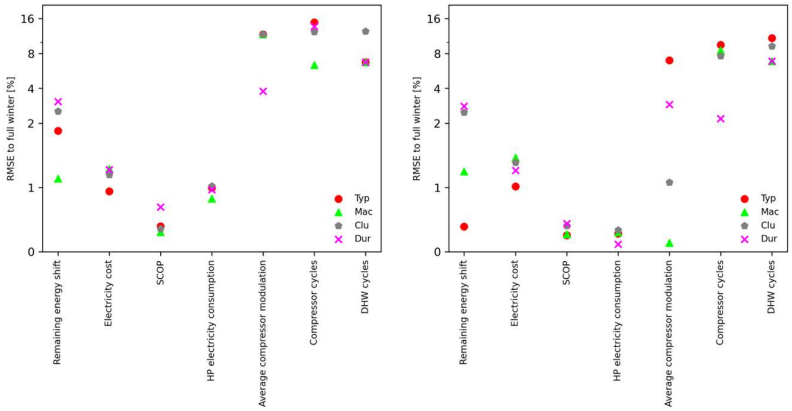

Figure 10 – RMSE according Eq. (11) for relative KPIs compared to full winter simulation for the Belgian Climate. Left: no SH TES between HP and building, right: HP – SH TES – building configuration

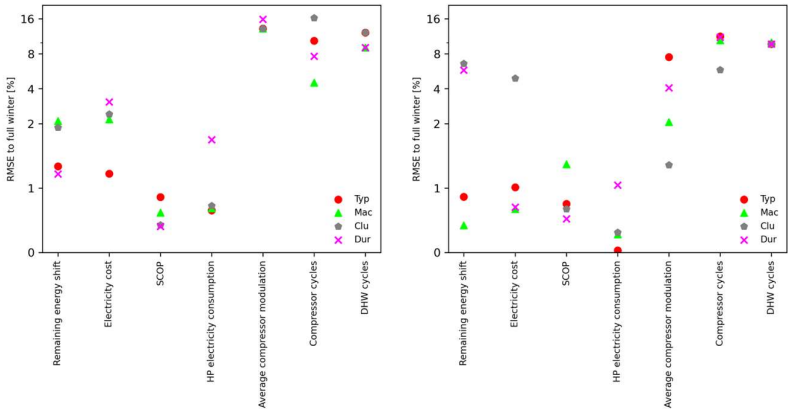

Figure 11 – RMSE according Eq. (11) for relative KPIs compared to full winter simulation for the Greek Climate. Left: no SH TES between HP and building, right: HP – SH TES – building configuration

To further analyse the performance of Mac and Typ over all control strategies, Figure 9 – Figure 11 show the $RMSE$ values according to Eq. (11) for several relative KPIs within the energy flexibility analysis, for the Finnish, Belgian and Greek climate, respectively. A logarithmic axis was used to better represent both small and large deviations. Again, the approaches Typ and Mac show only small deviations compared to Clu and Dur approaches. Energy-related KPIs such as the SCOP, remaining energy shift, energy cost and electricity consumption can be reasonably well represented with deviations mainly around 1 % and a maximum of 5 %. The consecutive day approach Typ performs mainly slightly better for cases without a SH TES, while Mac performs better when using a SH TES. It should be noted that the days within the energy-based day selection approach were selected when not using a SH TES. Hence, it was expected that the approach Mac should perform better than Typ for the hydraulic configuration without a SH TES. Higher deviations can be found for the HP operation indicators such as the average modulation capacity, compressor cycles and DHW cycles. Reasons can be found in the different environmental characteristics of the composed representative cycles as they affect the operational behaviour of the HP system.

Finally, energy flexible control strategies acting on SH services should also consider potential thermal discomfort. Figure 12 – Figure 13 provide the duration curves of the operative room and air temperature of the ground floor for the Belgian climate when not considering a SH TES between HP and building, respectively. The duration curves are similar for the Finnish and Greek climate, though less variation can be noticed. Potentially, a larger variability in weather conditions within the Belgian climate can be pointed out as a main reason when selecting non-consecutive days. The temperature duration curves are also similar for a hydraulic configuration with a SH TES between HP and building. Within these temperature duration curves, the full winter simulations can be compared to each representative day selection procedure for each HP control strategy. Again, the approaches Clu and Dur do not accurately represent the duration curves, especially when close to the discomfort band of an operative temperature of 19.5 °C. While the procedures of Typ and Mac show similar curves, the procedure Typ reaches a better overall agreement, especially when analysing the change in room temperature between the strategies REF and STRAT3. The effect of selecting non-consecutive days within the approaches Mac, Clu and Dur can be seen for both the operative and air temperatures. Herein, the potential thermal discomfort at the lower temperature ranges cannot be correctly represented when using non-consecutive days. Due to the thermal building inertia, these changes are better visible within the air temperature, but also at the level of the operative room temperatures. Hence, even by reducing the outdoor temperature transitions between non-consecutive days via Eq. (4), potential SH discomfort issues cannot be clearly tracked. Therefore, it can be concluded that both approaches Mac and Typ can be used for selecting representative days for energy flexibility analysis in time-shortened test cycles when only focussing on the energy performance. Though, it is recommended to use the consecutive day approach Typ when applying control strategies acting on the thermal building inertia or when applying control strategies for which the potential SH discomfort should also be incorporated.

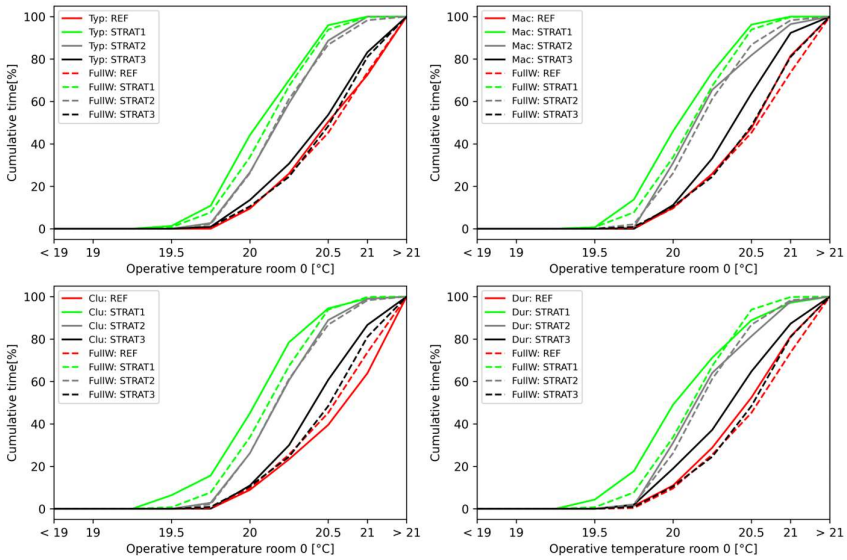

Figure 12 – Ground floor operative temperature duration curves for Belgium: representative day selection procedures (solid line) compared to full winter period simulation (dashed line). Left top: Typ, left bottom: Clu, right top: Mac, right bottom: Dur.

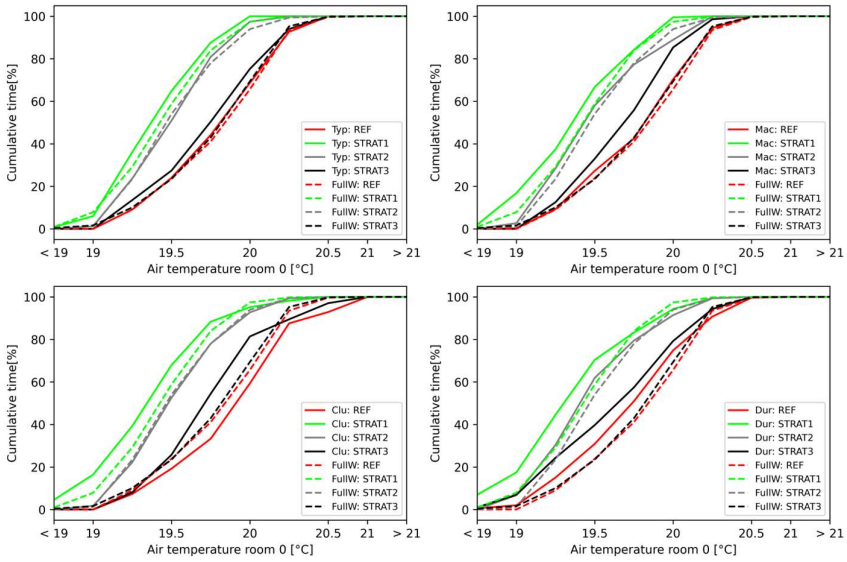

Figure 13 – Ground floor air temperature duration curves for Belgium: representative day selection procedures (solid line) compared to full winter period simulation (dashed line). Left top: Typ, left bottom: Clu, right top: Mac, right bottom: Dur.

3.3. Energy state correction mechanism

This section discusses the energy correction mechanism, used to achieve comparable state-of-charge conditions between the start and end of the test cycles. Within this context, detailed result analysis showed the necessity to correct the obtained thermal energies, electrical energies and energy costs after completing the simulation. Calculating the thermal energy difference via the state-of-charge of the building and thermal storages between the end of the initialisation day and end of the full test cycle according Eq. (8) provided a range between -25.68 kWh and 19.86 kWh. Incorporating the SCOP, an equivalent electricity consumption range of -4.24 kWh and 3.24 kWh could be found. With a total electricity consumption range between 81.66 kWh and 146.49 kWh over the three climatic zones,

comparison of the control strategy effectiveness led to wrong conclusions, especially when analysing small control strategy improvements. Indeed, some control strategies heated the building to higher temperatures during the end of the test cycle, which increased the electricity consumption. While the test cycle stops after eight days, the stored energy within the building has still an economical value that causes the need to correct the related cost and required energy consumption. Herein, comparison between several cases showed that when looking into the energy cost at the end of the test cycle without an energy state correction mechanism, it could be concluded that some of the control strategy improvements were not effective as they increased the energy cost and energy consumption. In contrast, when the profiles of the energy cost and energy consumption were compared throughout the full period, these strategies proved to be more effective in both cost and energy consumption. It could be seen that the decision of some control strategies to preheat the high thermal inertia building during the last test day consumed additional energy, while other strategies kept the building at lower temperatures and incomparable state-of-charges were reached. Within this context, Figure 14 shows the operative room temperature for both floors of a full test cycle, including the initialisation day and an indication of the energy differences for both floors. Herein, the difference in state-of-charge between the start and end of the test cycle for both floors is indicated by Δ0 and Δ1. The application of the energy state correction mechanism as a post-experimental or post-simulation measure aims to virtually eliminate the energy state differences Δ0 and Δ1 by applying a correction on the thermal energies, electrical energies and energy costs.

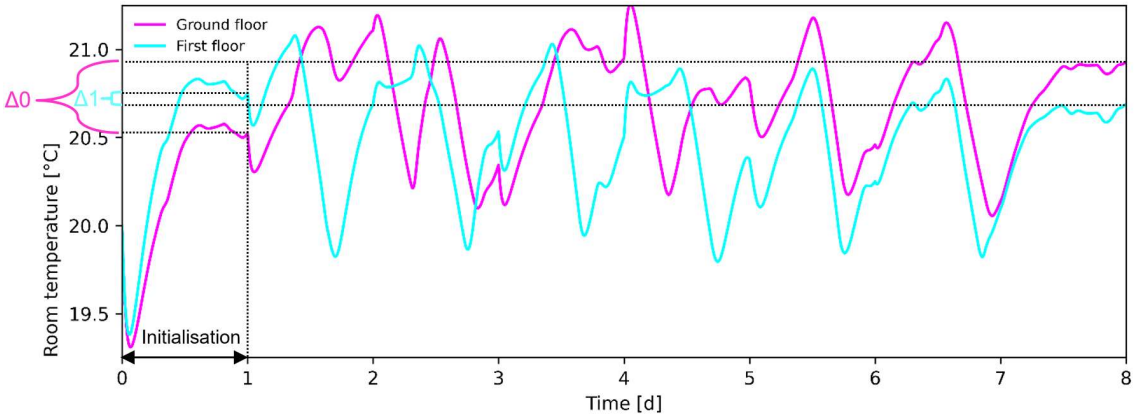

Figure 14 – Operative room temperature for ground floor (pink) and first floor (blue) with indicated energy difference for both floors (Δ0 and Δ1) between the end of the initialisation day and the end of the test cycle.

4. Discussion

In this work, we compared the applicability of several existing representative cycle approaches for energy flexibility analysis with heat pumps. A new approach, in which only consecutive days are used, was also evaluated. The main aim was to find the best selection approach for future use within hardware-in-the-loop experiments. Therefore, the selected representative cycle simulations were compared to full winter simulations for several key performance indicators. These indicators consider the full evaluation period and hence represent an average performance. In contrast, energy flexibility services vary throughout the winter season due to a variability in weather conditions. Better representing the variability in weather conditions was also evaluated within the Dur approach. Within this approach, days were selected to optimally match the duration curves of the outdoor temperature and global horizontal irradiation of the full winter season. Although the Dur approach represents a wider variability in environmental conditions, the analysis also showed a reversed effect on the energy flexibility analysis when compared to the full winter simulations. For instance, the building response,

energy cost reduction and energy consumption could not be accurately represented. A first reason is the adoption of non-consecutive days, which does not correctly represent the amount of shifted energy when switching between days, especially when concatenating days with extremer weather conditions. In addition, considering a wider variability in environmental conditions puts more stress on extreme outdoor conditions which do not often occur. Therefore, the authors recommend to use the consecutive day approach for energy flexibility analysis as it allows to obtain insights into both the average performance during the entire winter season and into the detailed heat pump and building behaviour.

Furthermore, this paper considered a novel approach to correct the building's state-of-charge at the end of the test cycle and to achieve comparable end conditions over several simulations. Herein, details from the building structure were used to identify the building's thermal mass. Depending on the level of simulation detail or even experimental equipment, these characteristics could also be derived via data driven approaches. The main principle of the energy correction approach can then still be used, but a thoughtful choice on which building elements should or should not be incorporated within the energy correction approach has to be made when simplifying the building model. It is recommended to only use the thermal inertia of insulated building elements. In addition, active heating layers should be carefully incorporated due to their high thermal inertia and weight within the energy correction mechanism.

Finally, this paper investigated several flexible heat pump control strategies solely under a dynamic pricing framework. While other flexibility signals or strategies such as CO_2 prices, peak shaving, optimisation of self-consumption, … were not considered, the authors believe that the suitability of the consecutive day approach and drawn conclusions will not be affected. Firstly, the day selection approach was not based on the flexibility signal itself, but on the environmental conditions or reference simulation without energy flexibility services. Secondly, the investigated control algorithms on the dynamic tariffs are considered as a milder strategy without extreme control decisions such as peak shaving strategies. Hence, the authors expect that applying a model predictive controller on the dynamic tariffs or applying a peak shaving strategy can even shift results to a stronger preference for considering a consecutive day selection procedure. Therefore, a future work could focus on evaluating the consecutive day selection procedure under a wider variety of flexibility signals.

5. Conclusion

This paper investigated the representative cycle requirements and day selection procedures when composing a time shortened, though representative, period for energy flexibility analysis with heat pumps during the winter season. Therefore, existing methodologies for retrieving yearly energy performance indications under normal operating conditions were compared to an alternative approach for which only fully consecutive days were used. In order to reach a general conclusion, the analysis was performed for a cold, average and warm European climate and for a total of seven heat pump control strategies. Moreover, two hydraulic configurations were tested, i.e. coupling the heat pump directly to the building or using a thermal energy storage between heat pump and building. Results showed that clustering days or selecting days to optimally represent the duration curves of the environmental conditions can only reach moderate results. Herein, two main reasons were found, i.e. (1) reaching an incorrect representation of the building response when switching between days, especially when concatenating days with extremer weather conditions and (2) by considering a wider variability in environmental conditions, more stress is put on extreme outdoor conditions which do not often occur. Therefore, applying day selection approaches based on day clustering or duration curve construction led to invalid conclusions when investigating control strategy improvements.

Furthermore, results showed that selecting consecutive days based on the average environmental conditions or selecting days based on the average energy consumption reached good agreements with full winter simulations. Herein, these two approaches focus more on better representing an average winter season instead of representing a wide variety of conditions. Results also showed that approaches which work with non-consecutive days encounter issues on correctly representing the thermal comfort due to potentially large temperature variations when switching between days. In this regard, non-consecutive approaches could not achieve a realistic building response and hence, a light preference for using consecutive days when solely acting on the energy flexibility of the thermal building inertia could be seen. Moreover, the comparison of the hydraulic configurations revealed a better agreement with the full winter simulations when using a thermal energy storage between heat pump and building. Herein, dividing the heat pump operation into thermal energy storage charging and discharging cycles allowed to limit the effects of changing environmental conditions and flexibility requests on the thermal response of the building. Finally, this paper proposed an energy state correction mechanism to incorporate the difference in state-of-charge of the building and storage between the start and end of the test cycle. Therefore, the mechanism ensures to reach comparable start and end conditions when comparing several control strategies and to draw correct conclusions.

Acknowledgement

This research work was funded by the Internal Funds KU Leuven.

We also thank Daikin for providing part-load performance data for the water/water heat pump type EGSAX06D9W.

References

[1] European Commission, “Factsheet - Energy Performance of Buildings,” 2021. [Online]. Available: https://ec.europa.eu/commission/presscorner/detail/pt/fs_21_3673.

[2] A. Arteconi and F. Polonara, “Assessing the demand side management potential and the energy flexibility of heat pumps in buildings,” *Energies*, vol. 11, no. 7, pp. 1–19, 2018, doi: 10.3390/en11071846.

[3] “EN 14511-3:2018 - Air conditioners, liquid chilling packages and heat pumps for space heating and cooling and process chillers, with electrically driven compressors - Part 3: Test methods,” 2018.

[4] “EN 14825 - Air conditioners, liquid chilling packages and heat pumps, with electrically driven compressors, for space heating and cooling. Testing and rating at part load conditions and calculation of seasonal performance,” 2018.

[5] J. Clauß and L. Georges, “Model complexity of heat pump systems to investigate the building energy flexibility and guidelines for model implementation,” *Appl. Energy*, vol. 255, no. May, p. 113847, 2019, doi: 10.1016/j.apenergy.2019.113847.

[6] M. Evens and A. Arteconi, “Influence of Internal Control Simplifications in Heat Pump System Modelling for Energy Flexibility Evaluations,” in *Proceedings of Building Simulation 2021: 17th Conference of IBPSA*, 2021, pp. 1–8.

[7] M. Evens and A. Arteconi, “Hardware-in-the-loop heat pump model validation for flexibility evaluations,” in *Proceedings of the 14th REHVA HVAC World Congress*, 2022, pp. 1–8.

[8] C. Palkowski and A. Simo, “Quick seasonal performance testing for heat pumps,” *Eceee Summer Study Proc.*, vol. 2019-June, no. 2016, pp. 1547–1552, 2019.

[9] R. Haberl, M. Y. Haller, P. Papillon, D. Chèze, T. Persson, and C. Bales, “Testing of combined heating systems for small houses : Improved procedures for whole system test methods,” no. Deliverable 2.3, pp. 1–50, 2015.

[10] D. Chèze *et al.*, “Towards an Harmonized Whole System Test Method for Combined Renewable Heating Systems for Houses,” no. September 2014, pp. 1–10, 2015, doi: 10.18086/eurosun.2014.03.06.

[11] D. Menegon, G. Cortella, O. Saro, and R. Fedrizzi, “Development of a Dynamic Test Procedure for the Laboratory Characterization of Thermally Driven Devices,” no. April, p. 2013, 2013.

[12] P. Mehrfeld, K. Huchtemann, and D. Müller, “Influences of hot water tank states and the order of test days to gain the annual efficiency of heat pump systems evaluated using modelica,” *Build. Simul. Conf. Proc.*, vol. 3, no. November 2019, pp. 1293–1298, 2017, doi: 10.26868/25222708.2017.396.

[13] K. Poncelet, H. Hoschle, E. Delarue, A. Virag, and W. D’haeseleer, “Selecting representative days for capturing the implications of integrating intermittent renewables in generation expansion planning problems,” *IEEE Trans. Power Syst.*, vol. 32, no. 3, pp. 1936–1948, 2017, doi: 10.1109/TPWRS.2016.2596803.

[14] L. Kotzur, P. Markewitz, M. Robinius, and D. Stolten, “Time series aggregation for energy system design: Modeling seasonal storage,” *Appl. Energy*, vol. 213, no. October 2017, pp. 123–135, 2018, doi: 10.1016/j.apenergy.2018.01.023.

[15] B. van der Heijde, A. Vandermeulen, R. Salenbien, and L. Helsen, “Representative days selection for district energy system optimisation: a solar district heating system with seasonal storage,” *Appl. Energy*, vol. 248, no. April, pp. 79–94, 2019, doi: 10.1016/j.apenergy.2019.04.030.

[16] P. Nahmmacher, E. Schmid, L. Hirth, and B. Knopf, “Carpe diem: A novel approach to select representative days for long-term power system modeling,” *Energy*, vol. 112, pp. 430–442, 2016, doi: 10.1016/j.energy.2016.06.081.

[17] KMI, “Klimaatstatistieken van de Belgische gemeenten,” pp. 1–6, 2015.

[18] FMI, “Seasons in Finland.” https://en.ilmatieteenlaitos.fi/seasons-in-finland.

[19] HNMS, “The Climate of Greece.” http://emy.gr/emy/en/climatology/climatology.

[20] M. Y. Haller *et al.*, “Dynamic whole system testing of combined renewable heating systems - The current state of the art,” *Energy Build.*, vol. 66, pp. 667–677, 2013, doi: 10.1016/j.enbuild.2013.07.052.

[21] U. Jordan, K. Vajen, and H. Braas, “DHWcalc: Tool for the Generation of Domestic Hot Water Profiles on a Statistical Basis (version 2.02b),” vol. 10, no. March, pp. 1–14, 2017.

[22] D. Menegon, A. Soppelsa, and R. Fedrizzi, “Clustering methodology for defining a short test sequence for whole system testing of solar and heat pump systems,” *ISES Sol. World Congr. 2017 - IEA SHC Int. Conf. Sol. Heat. Cool. Build. Ind. 2017, Proc.*, pp. 435–445, 2017, doi: 10.18086/swc.2017.08.03.

[23] D. Menegon, T. Persson, R. Haberl, C. Bales, and M. Haller, “Direct characterisation of the annual performance of solar thermal and heat pump systems using a six-day whole system test,” *Renew. Energy*, vol. 146, pp. 1337–1353, 2020, doi: 10.1016/j.renene.2019.07.031.

[24] H. Sayegh, A. Leconte, G. Fraisse, E. Wurtz, and S. Rouchier, “Computational time reduction using detailed building models with Typical Short Sequences,” *Energy*, vol. 244, p. 123109,

2022, doi: 10.1016/j.energy.2022.123109.

[25] D. Fischer, T. Wirtz, K. D. Zerbe, B. Wille-Haussmann, and H. Madani, “Test cases for hardware in the loop testing of air to water heat pump systems in a smart grid context,” *Refrig. Sci. Technol.*, no. April 2016, pp. 3666–3673, 2015, doi: 10.18462/iir.icr.2015.0584.

[26] R. Haberl, E. Frank, and P. Vogelsanger, “Holistic system testing - 10 years of concise cycle testing,” *29th ISES Bienn. Sol. World Congr. 2009, ISES 2009*, vol. 1, no. April 2014, pp. 351–360, 2009.

[27] Y. Ju, J. Jokisalo, R. Kosonen, V. Kauppi, and P. Janßen, “Analyzing energy flexibility by demand response in a Finnish district heated apartment building,” *E3S Web Conf.*, vol. 246, 2021, doi: 10.1051/e3sconf/202124609006.

[28] J. Schietecat, “Rapport 14: Ontwerp en dimensionering van centrale-verwarmings-installaties met warm water,” 2014. [Online]. Available: https://www.wtcb.be/homepage/download.cfm?dtype=publ&doc=WTCB_Rapport_14.pdf&lang=nl.

[29] G. Mouzeviris, K. Lagouvardos, and K. T. Papakostas, “Air-to-water heat pumps’ seasonal performance for heating in 16 Greek locations with climate data of the last decade,” *IOP Conf. Ser. Mater. Sci. Eng.*, vol. 1262, no. 1, p. 012084, 2022, doi: 10.1088/1757-899x/1262/1/012084.

[30] “Technical Data EGSAH/X series Daikin,” Oostende, 2020.

[31] F. Jorissen, G. Reynders, R. Baetens, D. Picard, D. Saelens, and L. Helsen, “Implementation and verification of the IDEAS building energy simulation library,” *J. Build. Perform. Simul.*, vol. 11, no. 6, pp. 669–688, Nov. 2018, doi: 10.1080/19401493.2018.1428361.

[32] D. Fischer and H. Madani, “On heat pumps in smart grids: A review,” *Renew. Sustain. Energy Rev.*, vol. 70, no. November 2016, pp. 342–357, 2017, doi: 10.1016/j.rser.2016.11.182.

[33] Elexys, “Belgian Day-Ahead electricity prices,” *Elexys*, 2020. .

[34] M. Lindahl, “Grid Flexible Control of Heat Pumps,” *HPT Mag.*, vol. 38, no. 1, pp. 31–34, 2020.